
Article:
Hartwich, D., Muller, G., Meierhofer, A.. et al. (4 more authors) (2022) A new hybrid approach to predict worn wheel profile shapes. Vehicle System Dynamics, 61 (6). pp. 1548-1564. ISSN 0042-3114

https://doi.org/10.1080/00423114.2022.2085585

A new hybrid approach to predict worn wheel profile shapes

Dietmar Hartwich[a]*, Gabor Müller[a], Alexander Meierhofer[a], Danijel Obadic[b], Martin Rosenberger[b], Roger Lewis[c] and Klaus Six[a]

[a] *Virtual Vehicle Research GmbH, Graz, Austria;* [b] *Siemens Mobility Austria GmbH, Graz, Austria;* [c] *The University of Sheffield, Department of Mechanical Engineering, Sheffield, UK*

*Dietmar Hartwich, dietmar.hartwich@v2c2.at

A new hybrid approach to predict worn wheel profile shapes

Abstract: Wheel maintenance is a complex process whose costs can be reduced with good planning. One of the main difficulties is the prediction of a worn wheel profile shape on a train. With existing modelling approaches, it is possible to predict a worn wheel profile quickly and accurately for a unique operating situation. For varying operating scenarios, it is a more time-consuming process and often less accurate manner because so many, sometimes even unknown, input data are needed. With the new hybrid approach developed in this work, it is possible to combine the advantages of both approaches (fast, accurate, varying operating scenarios). The hybrid approach builds on historical data sets of two trains in combination with multi-body dynamic simulations. In these simulations, two different wear models have been used, one based on the maximum shear stress, the other on the wear number in the contact point. The wear model approach based on the maximum contact shear stress was confirmed as accurate through application of the hybrid model and validation using real track measurements. This will help to improve the prediction of maintenance intervals and, thus, to reduce the costs.

Keywords: wear prediction; wheel profile prediction; hybrid approach; statistical wear prediction

1. Introduction

During operation, the shape of wheel and rail profiles can change due to wear. Depending on the materials, this can lead to large deviations from their initial profiles, which can cause, for example, noise, unwanted dynamics in the vehicle or issues with the steering behaviour. If the deviation from the initial profile is unacceptable, the wheels and rails are either reprofiled or switched. The resulting maintenance costs can be reduced if accurate profile prediction models are available. The development of such a model is a very complex task as many different influencing factors exist, e.g., the operating conditions of the train, rolling behaviour of wheel/rail, wear mechanism of the wheel/rail material and climatic influences.

Currently, two methods are widely used to predict worn wheel profiles [1], [2]. One

method is based on contact mechanics and is widely applicable to many scenarios. It has the disadvantage though of high computational effort, as well as often lower accuracy because so many, sometimes even unknown, input data are needed [3]. The other method is based on historical data sets. It is very accurate and fast, but can only be applied to one operating scenario. The intention of this work was to create a new method that quickly and accurately predicts the worn profiles for any scenario. For this purpose, first an overview is given of the two modelling approaches mentioned before. Then, the idea of a new, hybrid approach for wheel profile prediction is presented. The subsequent analysis of existing measurement data sets confirmed the assumptions of the hybrid approach. After the successful validation of the model, the results are then evaluated and conclusions are drawn.

1.1 State of the Art

Profile shape evolution caused by wear is currently typically predicted in one of two ways: using a method based on contact mechanics (1) or one based on statistical methods (2). The first method uses multi-body-dynamics (MBD) simulations and local wheel-rail contact analysis to obtain wheel-rail contact parameters (e.g.: slip, tangential forces, contact area) [3]-[4]. Based on these, material is locally removed according to the wear model being applied. This is followed by further MBD simulations with the updated wheel profiles in the next loop and so on (loop-based method), see Figure 1. This method is very time consuming, however, and needs a lot of input data to achieve realistic wear distributions across the wheel profile. These input data are difficult to determine or are even just not available. Also, simplifications and assumptions in the model lead to errors, which accumulate through thousands of wear superposition calculations. Smoothing algorithms during the stage where the wheel profile is updated add to this and the resulting total error can become quite large or even unacceptable. The advantage of this method,

however, is that other vehicle types or changing service conditions (curve radii distribution) can easily be considered.

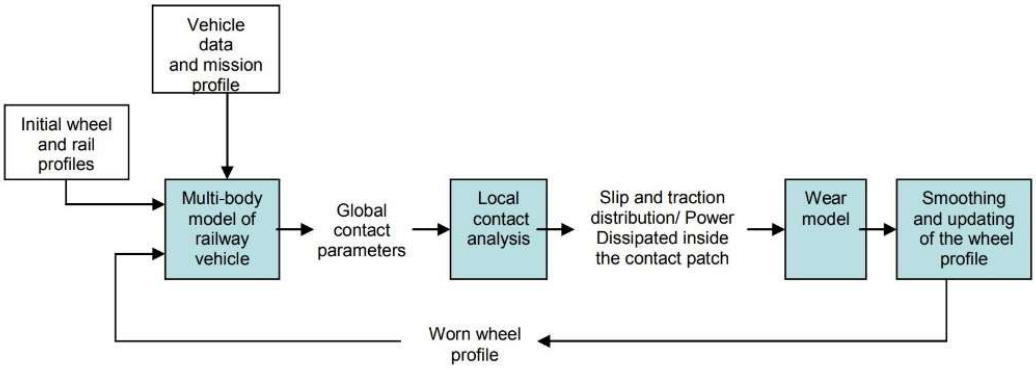

Figure 1 – Contact mechanics (loop) based wheel profile evolution prediction method [5]

In the contact mechanics based method, there are two frequently used wear modelling approaches for describing the wear in the wheel-rail interface, the Archard model [6], [7], [8] and $T\gamma$-approach [7], [9]-[10]. According to Archard, wear is described according to equation (1), in which the wear volume V is considered as being directly proportional to the load P as well as to the sliding distance l, but inversely proportional to the surface hardness H. This correlation is achieved via a parameter k, also known as material dependent wear coefficient [11].

$$V = \frac{k\,P\,l}{H} \qquad (1)$$

The $T\gamma$-approach is based on a wear number as the multiplication of the tractive force T and the contact slip γ. Several authors [12]–[14] have defined three different wear

regimes, see Figure 2. Each regime has its own wear coefficient. The coefficient depends on wheel-rail pairings, friction coefficients, materials, etc.

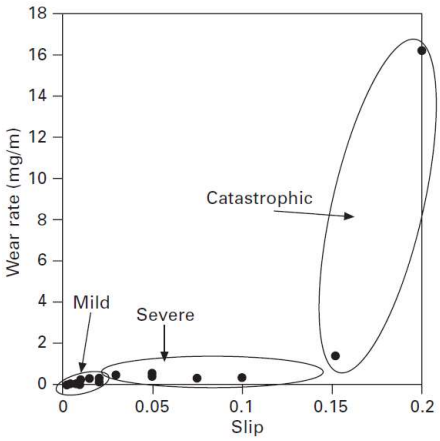

Figure 2 - Wear rates of R8T wheel material using a twin-disc rolling/sliding test [12]

While Archard and $T\gamma$ are well established, recently a new wear model based on the maximum contact shear stress τ_{max} has been developed. Al-Maliki et al. [13] found that the wear rate in the mild and severe regimes correlates better with the maximum shear stress τ_{max} in the contact patch, than with the wear number $T\gamma$ or Archard.

As an example of the contact mechanics based approach, Figure 3 shows the validation results from such a model created by Ding et al. [3]. The solid lines represent initial and predicted profiles and the dashed lines measured ones. As can be seen, simulation results do not match well with the actual profiles. For the outer wheel region, beginning at 30 to 40 mm, the simulated profiles show no wear while the measurements show that a relatively large amount of material removal has occurred here. The difference between the measured and predicted profiles is approximately 5 mm. The authors explain this discrepancy by the fact that they did not consider the rail switches and plastic deformation in the simulation. This confirms the statement that the accuracy of this approach depends on many uncertain input parameters which are sometimes even unknown.

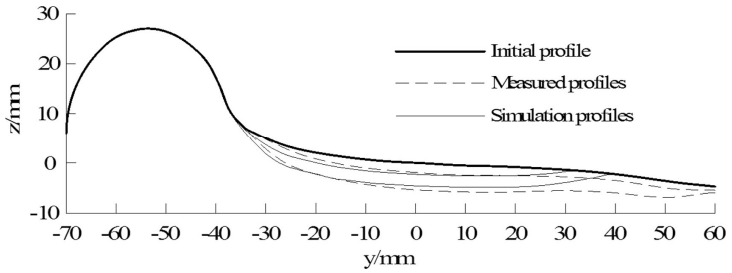

Figure 3 - Validation results from a contact mechanics based approach from Ding et al. [3]

The second widely used method for predicting the worn wheel profile shapes is based on historical data sets ([15], [16]). The measurements of worn profile shapes serve as a basis for the wear prediction. This, of course, only accounts for the influences of the operating conditions as they prevail during the measurement period. As soon as there is a significant change in the operating conditions (e.g. operation on track with a very different curve radii distribution), the prediction quality will drop. The main advantages of this method, however, are the short calculation time and high accuracy, but just for scenarios that are very similar to the data basis.

To illustrate the approach, the statistical wheel profile evolution model for high speed trains developed by Han and Zhang [15] is considered. Figure 4 shows their validation results from predictions carried out for a trailer bogie (first car) and a motor bogie (fourth car). In the model polynomials were fitted through each measured wear curve (S1-S9). In this work, wear curves are defined as the vertical distance between a reference (new) profile shape and a worn profile shape. The coefficients of these polynomials were then determined as a function of mileage. This allowed new wear curves to be predicted depending on mileage. As expected, the validation results do not show any strong deviations. As mentioned before, the model is not transferable to other operating scenarios; further measurement data would be necessary for this.

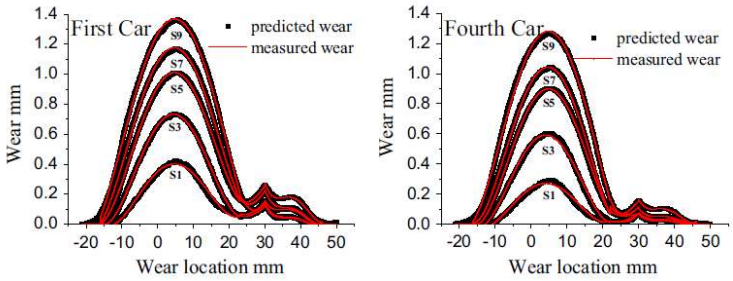

Figure 4 - Difference between predicted and measured wear curves for wheels from a trailer bogie (left) and a motor bogie (right) [15]

In the work described here, a new, hybrid approach is developed, which combines statistical and contact mechanics-based approaches to predict worn wheel profile shapes. The hybrid approach was used with both $T\gamma$ and τ_{max} wear models (used as relevant wear measures) to see which correlates better with actual wear development.

2. Methodology – Hybrid approach

The aim of the hybrid approach proposed for this work was to combine the statistical and the contact mechanics based methods and thus to use advantages of both (Figure 5).

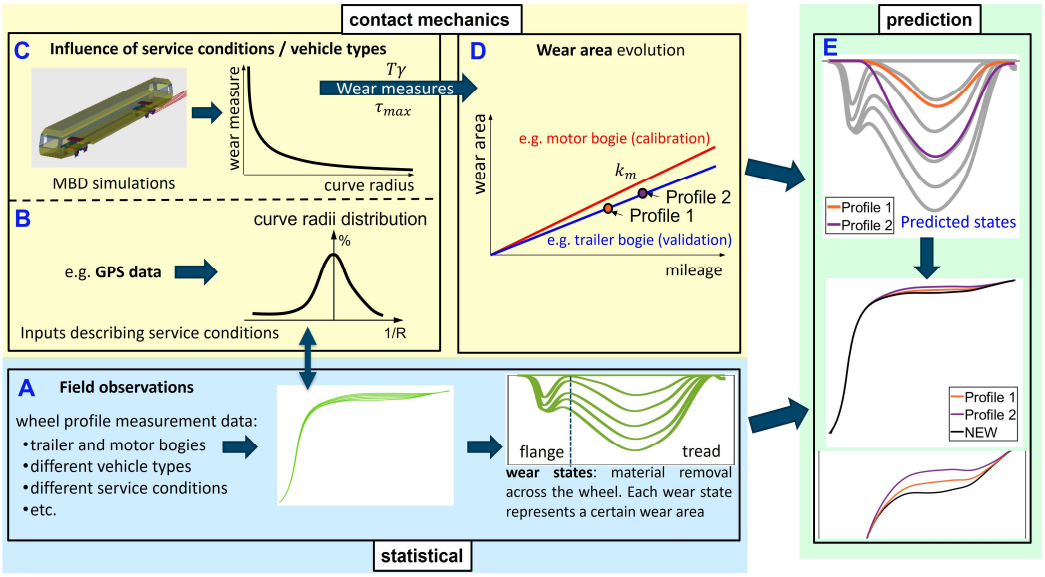

Figure 5 – Overview of the hybrid wheel profile evolution prediction approach

2.1 Statistical

The statistical part of the hybrid method (Figure 5 - A) includes profile shape measurements in the field, which are influenced by many, partly unknown factors (e.g. distributions of coefficient of friction, train payload, braking/traction and track properties). The wear curves of similar shape (as shown in Figure 4) and similar wear values are grouped separately for flange and tread independent of operating conditions and mileage. The average of each group is called the wear state. Each of these wear states has a corresponding wear area. If the dependency of wear area on milage is known, i.e. the wear rate, this can be used to interpolate between wear states and create the predicted wear curves for a given mileage. The wear rate can either be determined from measurements or MDB simulations, thus it can be different for different scenarios. In summary, the idea is that each wheel passes through the same wear states during operation, but, depending on the operating scenario, at different mileages.

2.2 Contact mechanics

This section presents the contact mechanics based part of the hybrid approach (Figure 5 – B, C, D) which is used to account for the influence of service conditions. Here, only the influence of the curve radii distribution on the track on which the vehicle is operated has been considered. MBD simulations for different curve radii are performed to get information about the relationship between curve radius and wear measures ($T\gamma$ and τ_{max}), as presented in Figure 5 - C. These simulations are performed with only one typical wheel-rail profile pairing (new profiles in this case), one typical coefficient of friction, one typical vehicle loading and one typical speed for each curve radius. This keeps the simulation effort as low as possible. It is not the quantitative values that are important here, but rather the characteristic behaviour and the change of the wear measures over

curve radii. The wear measure results P($T\gamma$) and P(τ_{max}) are calculated according to equation (2):

$$P = \sum_{i=1}^{n} c_i \, P_i \qquad (2)$$

where P_i is the wear measure for each scenario, c_i is the occurrence of a certain scenario (e.g., curve radius) and $i = 1,..n$ the number of scenarios for a vehicle.

A linear wear area evolution over mileage is assumed in the methodology (Figure 5 - D) based on the measurement. The according wear rate k_m, defined as wear area divided by mileage, depends on the vehicle type, friction in wheel-rail interface, operating conditions, etc. As an example, a passenger train operated on a curved track will show a very different wear rate compared to a high speed train which is operated mainly on tangent track and shallow curves. Another example is the different wear behaviour of wheels mounted on trailer and motor bogies in the same train, because of the different curving properties of the bogies. Each wear area corresponds to a wear curve. As already mentioned earlier, it is assumed that the same wear curve develops in both cases, but at very different mileages (because of different wear rates). This is because every wheel is in contact with many different rail profiles – rail profile collective – which in the end determines the wheel wear states. Because a wheel can typically come into contact with the rail at more than one point (e.g. two-point contact), flange and tread contacts are considered separately from each other resulting in flange and tread wear states. The wear rates of flange and tread are generally different and depend on the operating scenarios, e.g., there is more wear expected at flange in tighter curves.

2.3 Calibration

For model calibration, the wear rate k_m is determined based on available measured data from a train where the service conditions – in this work the curve radii distribution – are

known. Next, as described before, MBD simulations are performed for this train for the corresponding curve radii.

As mentioned in section 1.1, different wear models can be used in the contact mechanics based approach on the wheel-rail contact level. The widely used $T\gamma$-model is based on the traction force T and the slip γ, while the latest model by Al-Maliki et al. [13] takes the maximum shear stress τ_{max} in the contact patch as the most relevant wear measure. Both values are results of the MBD simulations performed. P_m in equation (3) represents the weighted wear measure, e.g., the curve radii distribution taken from measurements, calculated according to equation (2). It is assumed that the measured wear rate k_m can be linked to the weighted wear measure (P_m) by introducing a constant calibration factor c_s.

$$k_m = c_s P_m \qquad (3)$$

2.4 Prediction

This section describes the prediction part of the hybrid approach (Figure 5 – D, E). To apply the model to any operating scenario, the weighted wear measure (P_s) for a new scenario needs to be calculated by performing MBD simulations. Subsequently, the related new wear rate k_s is determined according to equation (4) by using the already calculated calibration factor c_s (3). Next the new wear curve can be calculated for any mileage (separately for flange and tread regions) by using the wear rate k_s. The individual wear curves for the flange and tread are then combined into a complete wear curve. The transition zone from the flange to the tread is smoothed out by using a moving average algorithm.

$$k_s = c_s P_s = k_m \frac{P_s}{P_m} \qquad (4)$$

3. Measurement data

Wheel profile measurements were performed on two identical electrical multiple units (EMUs). The two trains (train I and train II) were operated on slightly different routes and data from both types of bogies, i.e. motor bogie (MB) and trailer bogie (TB) were available for both trains. In the following, fictitious numbers are assigned to the bogies (MB/TB-x), these are to show that the measurements do not only come from one bogie. The measurement data analysis was carried out first using the data from train I, as these were available up to a higher mileage (210 tkm) than for train II (109 tkm). The data set of train I was used as the basis for the statistical part (Figure 5 - A) of the hybrid approach and the calibration as well. The measurement data of both trains were used for model validation.

In this section, the measured wear curves are first examined, then the influence of the train side and the bogie type on the wear development (wear area over mileage) is discussed. Finally, the determined wear states are presented.

3.1 Shape of wear curves

To evaluate the measurement data, wear curves were calculated as the vertical distance to the reference profile, following [15]. The reprofiling of MB-3 was done at a different date, so the measurements, which were taken on the same day for all wheels show an offset of approximately 20 tkm for MB-3 Hence, it was excluded from the shape comparison presented in Figure 6 and Figure 7. However, all measured data were used to evaluate the wear development.

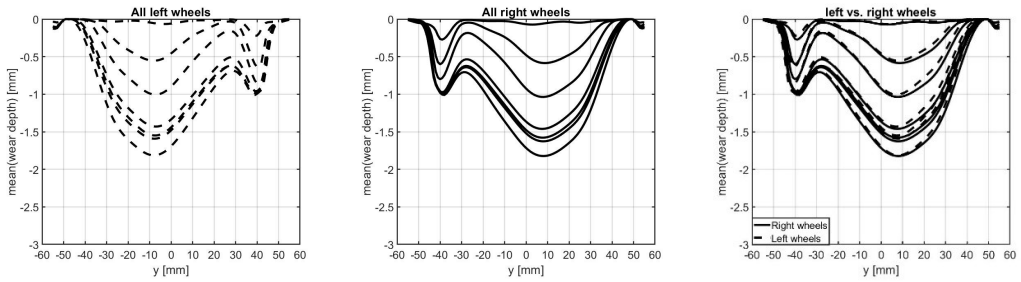

Figure 6 – Comparison of the averaged wear curves between left and right wheels (bogie and profile type independent)

The statistical approach of Han and Zhang [15] described in section 1.1 is based on wheel profile measurements (see wear curves in Figure 4) taken on different bogies from the same train. When looking at their measurement results, a similarity between all wear curves regarding their shape is noticeable (bogie type independent). A similar behaviour was observed when analysing the data of train I. Figure 6 shows the wear curves averaged for each given mileage of left and right wheels. The average includes data for all bogie types. Each wear curve has two maxima, which indicate the location where many contacts occur (tread and flange region). The minimum ($y \approx -30$ mm) of the wear curves refers to the transition zone between flange ($y < -30$ mm) and tread ($y >- 30$ mm). The exact position of the minimum varies slightly depending on the wear curve. Nevertheless, this variation was seen as insignificant as the wear in this area was at its lowest. Hence, the separation into flange and tread was set to y=-30mm for all wear curves.

The results also showed very similar wear behaviour, independent of vehicle side. While literature reports that asymmetrical curve radii distributions might lead to asymmetrically worn wear profiles and, therefore, asymmetrical wear curves [17], such behaviour was not found in this data and could not be regarded during the calibration and validation process in this paper. This is not surprising, as the curve radii distribution of the track on which the vehicle under investigation was operating is also more or less symmetrical. However, generally the presented methodology is able to consider asymmetric wear caused by an asymmetric curve radii distribution by the individual calculation of the wear

rate for the right and left sides of the train. This needs to be validated in future investigations.

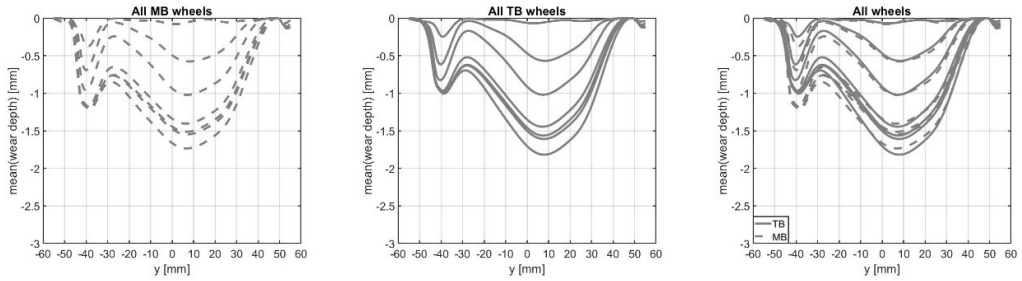

Figure 7 – Comparison of the averaged wear curves between MB and TB wheels (train side and profile type independent)

Figure 7 shows the averaged wear curves of MBs and TBs, train side independent. All curves show two maxima, these are approximately at the same position and for the tread have the similar height. The only visible difference is the height of the maxima at the flange.

In summary, the assumption that wheel profiles always pass the same wear states – separating tread and flange region – independent of the bogie type, and the train side (left/right) is supported by this analysis and by considering the results from the literature.

3.2 Wear area evolution

Figure 8 shows the averaged wear area development over mileage measured on MBs and TBs. As mentioned before in section 2.3, a linear relationship can be observed for all curves. TB curves show a slightly lower gradient than the MB curves.

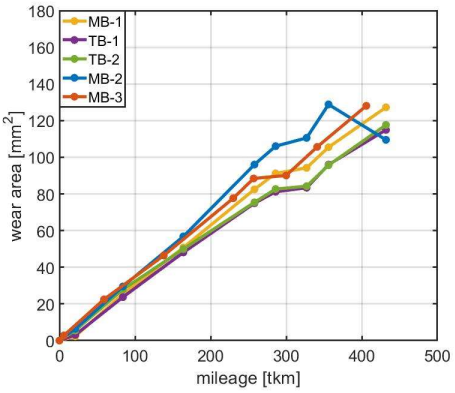

Figure 8 – Measured total wear area development over mileage for MBs and TBs: sum of tread and flange region

The profiles develop almost linearly with slightly different constant wear rates, but these small deviations have no significant influence on the related wear curves. It should be noted that all measurements were performed on the same date, however the MB-3 was reprofiled on a different day, leading to a difference in mileage compared to the other bogies and profile types. This confirms once again the assumption described previously, that the wear passes through the same wear states (see Figure 9), independent of the train side and bogie type. As described in section 2.1, the wear states have been calculated based on the wear curves shown in Figure 7.

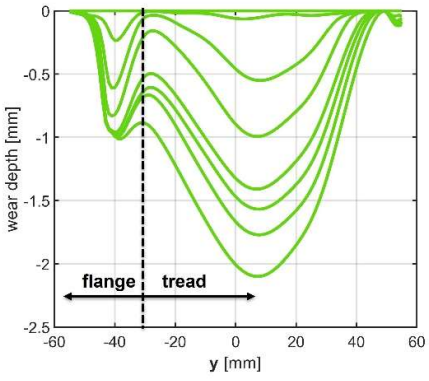

Figure 9 - Wear states calculated from wear curves

4 Calibration & Validation

The calibration of the methodology was carried out using the MBs of train I, while it was validated on the TBs of train I and train II. In the simulation, a bogie with two wheel-sets

was considered. Simpack 2020 was used for the MBD simulations to calculate the considered wear measures τ_{max} and $T\gamma$ at different curve radii derived from the routing of the trains. Because τ_{max} is not a direct output of Simpack 2020, it was calculated by dividing the maximum contact pressure (p_0) by the effective adhesion coefficient (μ_{eff}):

$$\tau_{max} = \frac{p_0}{\mu_{eff}} \quad (5)$$

Effects from traction and braking were not considered due to the large distances between stops and to keep the method as simple and practicable as possible. As already mentioned, each curve radius was simulated with only one representative speed (according to unbalanced lateral acceleration 0.58 m/s²), loading condition (loaded) and coefficient of friction (0.35) in the wheel-rail interface. Unworn wheel (initial profile S1002) and rail profiles (60E2 from the EN 13674 – 1 standard) were used for all the simulations.

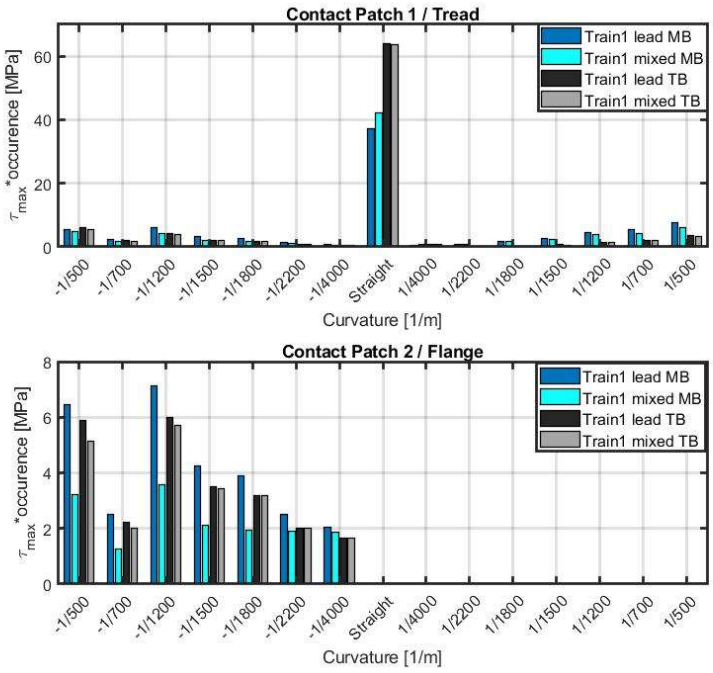

(a)

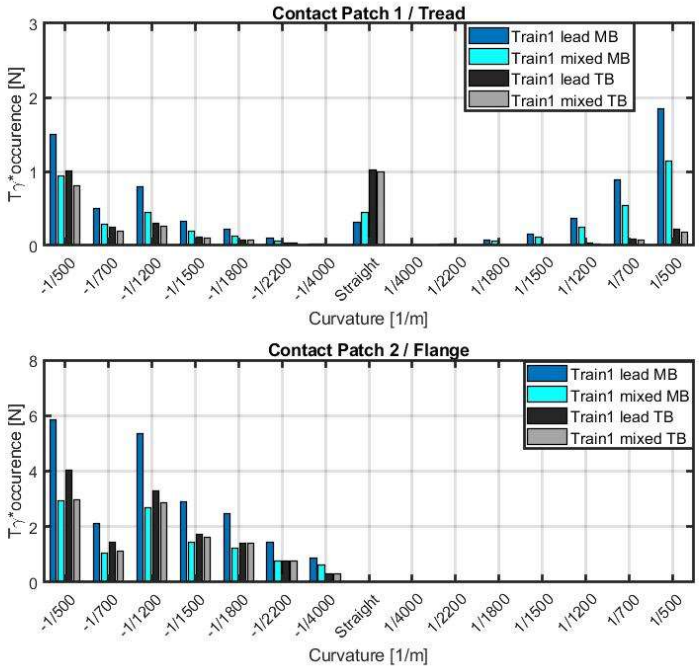

(b)

Figure 10 - Weighted maximum wheel-rail contact shear stress (τ_{max}) and wear number (Tγ) as a function of curve radius for tread (upper plot) and flange contacts (lower plot).

Figure 10 shows the calculation of P_m assembling of the track using the wear measures τ_{max} (Figure 10 - a) and $T\gamma$ (Figure 10 - b) with the occurrence of the curve radii on the track, according to equation (2). The results for both, TBs and MBs, are shown. Tread (upper plots in Figure 10) and flange contacts (lower plots) are plotted separately. Negative curvature means that the wheel runs on the high rail, positive curvature corresponds to the wheel running on the low rail.

The results for the leading wheel-set (first wheel-set) where thought to be representative for all leading axles of all bogies, while the trailing wheel-set (second wheelset) was thought to be representative of all trailing wheel-sets.

To investigate the influence of the running direction of the bogie, a distinction is made between “lead” and “mixed”. “Lead” means that the train is only operated in one direction and the considered wheelset is always in the leading position while “mixed” means that the train is operated in both directions (considered the wheelset is 50% in the leading position and 50% in the trailing position). This was done because it was not possible to identify the manner in which the train changed its direction (reversal at terminus stations versus round-trips). The exact position of the wheel-set (1st versus 3rd versus 5th wheel-set) was assumed to be less significant and, thus, neglected. As shown in Figure 10, there is a significant difference between “lead” and ”mixed”. Both, results for “lead” and “mixed” are presented in Figure 11.

As mentioned before, calibration was performed on the MBs of train I and the value of c_s determined according to equation (3). To validate the model, the c_s from the calibration was used to predict the wear behaviour of TBs of the same train. This was first done based on the wear rate (Figure 11). The dashed lines show the measurement corridor in which the TB measurement results scatter (all points are in the corridor). The red line is the regression through all wear area measurements carried out on the TB wheels. The

spin is low in the tread region, so its influence is neglected in the model. Although spin has a greater role in the flange region than in the tread region, it is neglected due to the low wear in the flange region. A clear difference between the predictions based on τ_{max} and $T\gamma$ can be seen in the results for the tread (left plot). The τ_{max}-based method is not only within the measurement corridor, but also very close to the regression line. In contrast, the "lead" and "mixed" $T\gamma$-based predictions are outside the measurement corridor. A large difference between "lead" and "mixed" $T\gamma$-based predictions is also noticeable, whereas the τ_{max}-based predictions are very close to each other. Thus, the running direction has no great influence on the tread wear of the τ_{max}-based prediction.

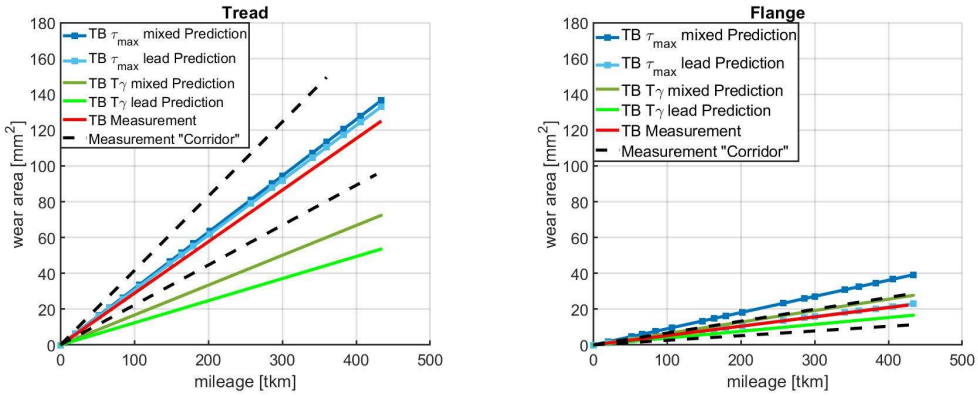

Figure 11 – Predicted wear area development over mileage in the tread and flange region for TBs of train I and comparison with measurement data.

For the flange, the τ_{max}-based prediction for the "mixed" case is outside the measurement corridor, while the "lead" case is almost at the red line. The two $T\gamma$-based predictions for the flange region are both within the measurement corridor. Due to the low wear values at the flange region compared to the tread region, small alignment issues have a high impact on the results. Thus, the predictions and the measurements in the flange region are considered as less reliable than those on the tread. Due to the very low wear in the flange region, the validation of the shape of the worn profiles is performed exclusively for the tread region.

In the following, the validation is carried out on a profile level. Therefore, several wheels from train I and train II are considered. For train I, track data to determine the curve radii distribution were available up to 201 tkm. While the wheel profile measurements were available for the first 432 tkm. This allows a reliable validation of the methodology up to 201 tkm. Because the wear rate did not change it was assumed that the train continued to travel more or less on the same route. For train II, there was track data available up to 109 tkm while profile measurements were available up to 404 tkm. Here, too, the validation was performed based on the assumption that the train was operated on the same route after 109 tkm. A validation at 109 tkm for train I is not very meaningful due to the low wear values, as the differences between the two methods would not be apparent.

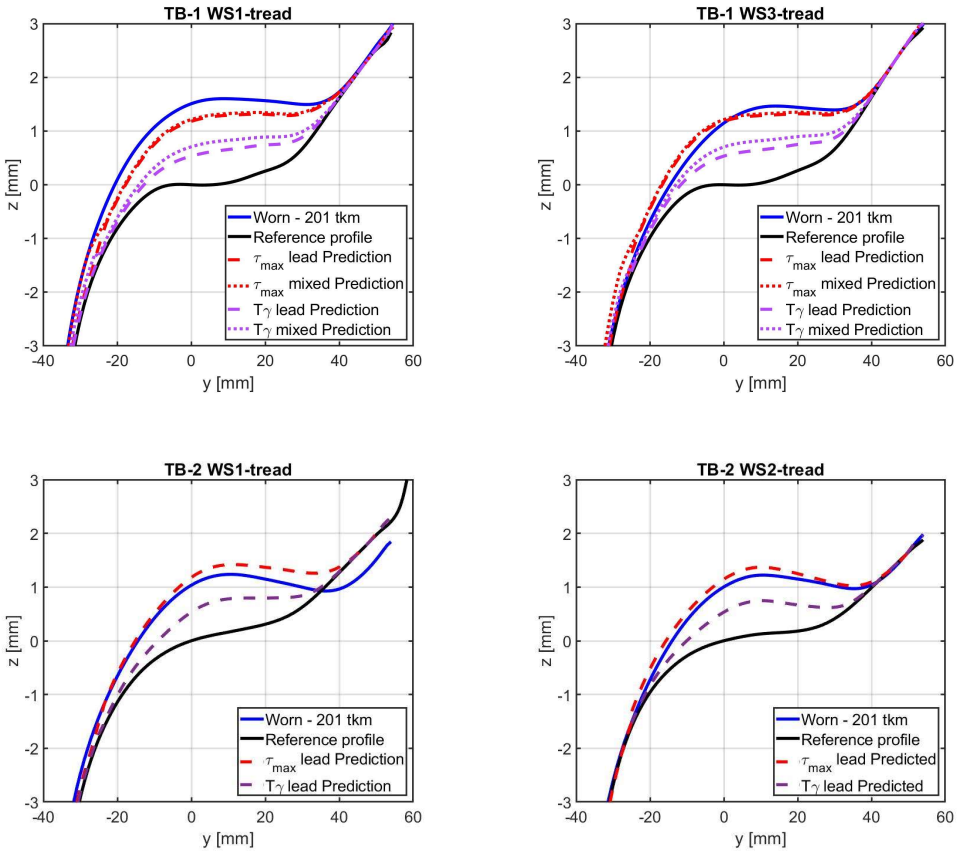

Figure 12 – Profile validation on train I at 201 tkm

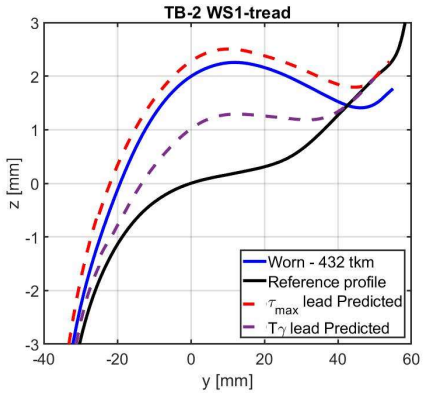

Figure 13 – Profile validation on train I at 432 tkm

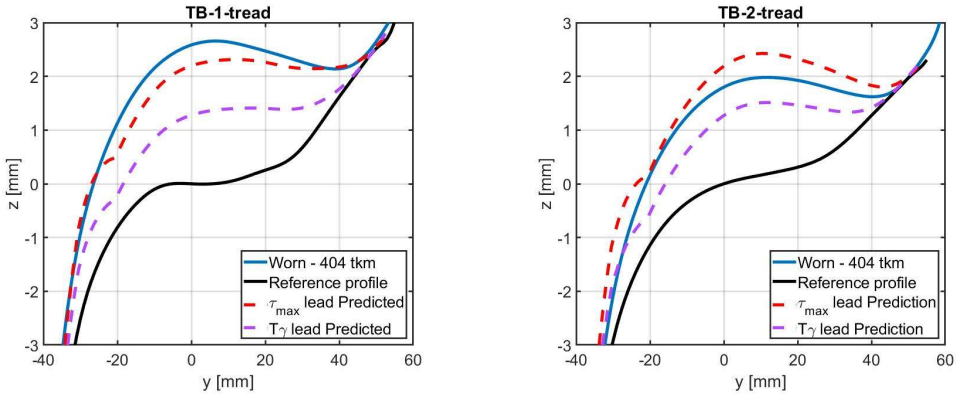

Figure 14 – Profile validation on train II at 404 tkm

Figure 12, Figure 13 and Figure 14 show prediction results together with measurement data for selected wheels. The following evaluation refers only to the tread region. As already mentioned above, the wear in the flange region is too low to be able to draw reliable conclusions. Figure 12 shows predictions for four wheel profiles on train II. In all cases, the τ_{max}-based predictions are closer to the measurement than $T\gamma$-based predictions. Furthermore, as in Figure 11, there is almost no difference between the "lead" and "mixed" cases in the τ_{max}-based predictions (upper two plots). The extrapolation to 432 tkm depicted in Figure 13 shows the same behaviour as in Figure 12 meaning that the τ_{max}-based predictions are closer to the measurement than $T\gamma$-based predictions. The same is true for the results of TB-1 from train II presented in Figure 14, while the results for TB-2 show a similar deviation for τ_{max} and $T\gamma$.

The presented results reveal that τ_{max}-based predictions show a better agreement with the measurement results than $T\gamma$-based predictions. This is caused by differences regarding the weighted wear measure ratio P_s/P_m based on τ_{max} and $T\gamma$ according to equation (4). For example, in the tread region the ratio P_s/P_m based on τ_{max} is close to 1 (no big difference between MB and TB wear rates as the measurements showed) while in the $T\gamma$ based case it is around 0.5 (MB has about twice the wear rate of TB). The main reason for this behaviour can be seen in the top plots of Figure 10. In the case of τ_{max} (left), the sum of all bars for the MBs (either "lead" or "mixed") is nearly the same as for the TBs (ratio around 1) while in the case of $T\gamma$ (right) this sum is very different (ratio around 0.5). The big difference between MBs and TBs in the case of $T\gamma$ is dominated by the big difference of the $T\gamma$ values in the 500 and 700 m curves when the wheel runs on the high rail.

To summarise, τ_{max}-based predictions show a good agreement with the measurement data, while $T\gamma$-based predictions show larger deviations. This is in good agreement with observations Al-Maliki et al. [13] made on wear results from twin disc experiments which further strengthens this approach.

5. Model application

Figure 15 shows an application example on a tangent track of the calibrated and validated hybrid methodology to a TB (two wheel profiles) together with the results from the real operating conditions as shown before. For the application, the same calibration factor c_s has been used as for the validation. When running on a tangent track, the contact with the rail takes place only on the tread, which means that only the tread wears out. The flange remains untouched, so that no wear occurs there. The blue curves in Figure 15 represent measurements for the comparison of the worn profile shapes between a curved (blue) and a simulation that assumes 100% tangent track (red). The results show a significant

increase in tread wear because contact occurs only in the wheel tread region in this case. On the other hand, the wear in the flange region disappears. It is worth noting that the calculation effort is a simple table evaluation and therefore almost instant, which highlights the benefit of the method. Due to the change of the operating scenario, such a prediction is not possible with a purely statistical based approach. A purely contact mechanics-based method would allow prediction of the profile evolution for such a new scenario, but this would lead to a very long calculation time. Furthermore, the prediction quality of such a contact mechanics-based method depends highly on the needed input data, which are often just not available. The new hybrid approach presented in this work does not have this issue.

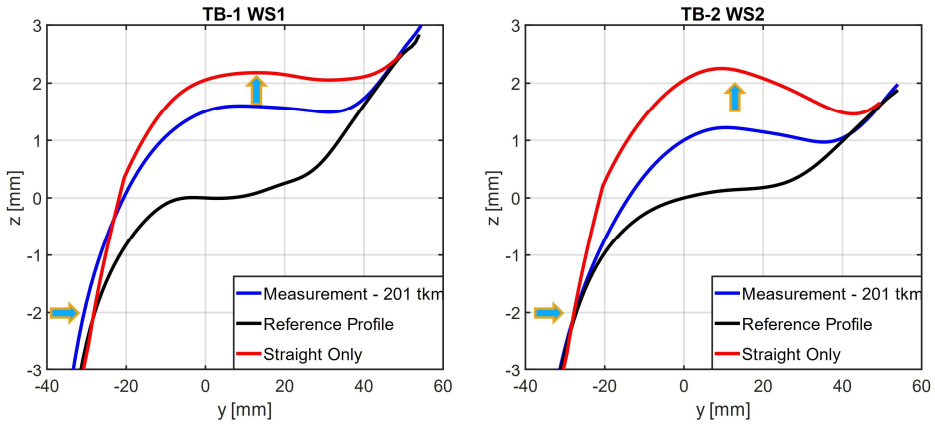

Figure 15 – Comparison of model results using a measured profile vs. a simulation that assumes a curve distribution of 100% tangent track

6. Conclusion

A new hybrid methodology for the prediction of worn wheel profiles was developed by combining statistical and contact-mechanics based methods. The goal was to develop a practical tool that can reliably predict wheel wear.

In contact mechanics based methods, different models can be used to describe the wear behaviour on contact level. A new approach, based on the maximum shear stress in the contact patch (τ_{max}) was used in this work and compared with a $T\gamma$-based approach. This

comparison was done based on wheel profile measurement data of two trains. After the model was calibrated on MBs of the first train, it was successfully validated on the TBs of both trains. Using τ_{max} as wear measure on contact level as part of the hybrid methodology, the agreement with the measurement results was similar or better than a $T\gamma$-based approach. This confirmed an assumption from the literature [13] that, at least for this type of train, the wear in the wheel-rail interface is mainly dominated by the contact shear stresses rather than the wear number. The applicability to different train types and further validations of the method are the focus of future research.

However, the influence of different wheel materials, considering the application of friction management products and accounting for effects from traction and braking which is important when the method is applied to locomotives have been not considered, therefore it is planned to extend the model in future work. This will help to improve more the prediction of maintenance intervals and, thus, to reduce the costs.

Acknowledgements

The publication was written at Virtual Vehicle Research GmbH in Graz, Austria, together with all listed co-authors. The authors would like to acknowledge the financial support within the COMET K2 Competence Centers for Excellent Technologies from the Austrian Federal Ministry for Climate Action (BMK), the Austrian Federal Ministry for Digital and Economic Affairs (BMDW), the Province of Styria (Dept. 12) and the Styrian Business Promotion Agency (SFG). The Austrian Research Promotion Agency (FFG) has been authorised for the programme management. They would furthermore like to express their thanks to their supporting industrial and scientific project partners Siemens Mobility GmbH, voestalpine Rail Technology GmbH and the University of Sheffield.

References

[1] A. Zhu *et al.*, “Research on Prediction of Metro Wheel Wear Based on Integrated Data-Model-Driven Approach,” *IEEE Access*, vol. 7, pp. 178153–178166, 2019, doi: 10.1109/ACCESS.2019.2950391.

[2] Y. Ye, Y. Sun, D. Shi, B. Peng, and M. Hecht, “A wheel wear prediction model of non-Hertzian wheel-rail contact considering wheelset yaw: Comparison between simulated and field test results,” *Wear*, vol. 474–475, no. June 2020, p. 203715, 2021, doi: 10.1016/j.wear.2021.203715.

[3] J. Ding, F. Li, Y. Huang, S. Sun, and L. Zhang, “Application of the semi-Hertzian method to the prediction of wheel wear in heavy haul freight car,” *Wear*, vol. 314, no. 1–2, pp. 104–110, 2014, doi: 10.1016/j.wear.2013.11.052.

[4] Z. Wang, R. Wang, D. Crosbee, P. Allen, Y. Ye, and W. Zhang, “Wheel wear analysis of motor and unpowered car of a high-speed train,” *Wear*, vol. 444–445, p. 203136, Mar. 2020, doi: 10.1016/j.wear.2019.203136.

[5] F. Braghin, R. Lewis, R. S. Dwyer-Joyce, and S. Bruni, “A mathematical model to predict railway wheel profile evolution due to wear,” *Wear*, vol. 261, no. 11–12, pp. 1253–1264, 2006, doi: 10.1016/j.wear.2006.03.025.

[6] H. K. Jun, D. H. Lee, and D. S. Kim, “Calculation of minimum crack size for growth under rolling contact between wheel and rail,” *Wear*, vol. 344–345, pp. 46–57, Dec. 2015, doi: 10.1016/j.wear.2015.10.013.

[7] R. Lewis *et al.*, “Towards a standard approach for the wear testing of wheel and rail materials,” *Proc. Inst. Mech. Eng. Part F J. Rail Rapid Transit*, vol. 231, no. 7, pp. 760–774, Aug. 2017, doi: 10.1177/0954409717700531.

[8] A. Ramalho, “Wear modelling in rail–wheel contact,” *Wear*, vol. 330–331, pp. 524–532, May 2015, doi: 10.1016/j.wear.2015.01.067.

[9] R. Chen, J. Chen, P. Wang, J. Fang, and J. Xu, “Impact of wheel profile evolution on wheel-rail dynamic interaction and surface initiated rolling contact fatigue in turnouts,” *Wear*, vol. 438–439, p. 203109, Nov. 2019, doi: 10.1016/j.wear.2019.203109.

[10] F. Salas Vicente and M. Pascual Guillamón, “Use of the fatigue index to study rolling contact wear,” *Wear*, vol. 436–437, p. 203036, Oct. 2019, doi: 10.1016/j.wear.2019.203036.

[11] R. Lewis and U. Olofsson, *Basic tribology of the wheel-rail contact*. Woodhead Publishing Limited, 2009.

[12] R. Lewis and R. S. Dwyer-Joyce, “Wear mechanisms and transitions in railway wheel steels,” *Proc. Inst. Mech. Eng. Part J J. Eng. Tribol.*, vol. 218, no. 6, pp. 467–478, Jun. 2004, doi: 10.1243/1350650042794815.

[13] H. Al-Maliki, A. Meierhofer, G. Trummer, R. Lewis, and K. Six, “A new approach for modelling mild and severe wear in wheel-rail contacts,” *Wear*, pp. 1–23, 2021.

[14] T. G. Pearce and N. D. Sherratt, “Prediction of wheel profile wear,” *Wear*, vol. 144, no. 1–2, pp. 343–351, 1991, doi: 10.1016/0043-1648(91)90025-P.

[15] P. Han and W. hua Zhang, “A new binary wheel wear prediction model based on statistical method and the demonstration,” *Wear*, vol. 324–325, pp. 90–99, 2015, doi: 10.1016/j.wear.2014.11.022.

[16] L. P. Lingaitis, S. Mikalunas, and V. Podvezko, “Statesticheskije imitazionije prognoznie modeli ozenok iznosa bandazhej kolesnich par lokomotivof,” *Transp. Telecommun.*, vol. 6, no. 3, pp. 391–396, 2005.

[17] R. D. Frohling, “Analysis of asymmetric wheel profile wear and its consequences,” *Veh. Syst. Dyn.*, vol. 44, no. SUPPL. 1, pp. 590–600, 2006, doi: 10.1080/00423110600879296.